

Effect of preparation temperature of titanium dioxide deposited on FTO glass on the UV photoresponse of photodetectors.

^{1,2} Basheer Kadhim Hassan Al-Mayyahi, ¹Mohammad Akbarzadeh Pasha and ³Husam S.Al-Salman

¹Faculty of Science, University of Mazandaran, Mazandaran, Iran.

²Directorate of Education in Al Basrah, Ministry of Education, Basrah, Iraq.

³Department of Physics, College of Science, University of Basrah, Iraq

Basheerkadhim38@gmail.com

makbarzadehpasha@gmail.com

husam.jasim@uobasrah.edu.iq

Abstracts

In this study, titanium dioxide (TiO₂) nanocomposite membranes were prepared Installation on FTO bases by hydrothermal method and at high temperatures (150°C , 160°C,170°C and 180°C) by holding the titanium dioxide concentration constant at 0.5 ml and time Constant deposition for 4h. These films were prepared by adding 0.5 ml. Of titanium butoxide (TiO₂), 20 ml of hydrochloric acid, and 20 ml of deionized water. Heat treatment was carried out at 450 °C for two hours , UV tests were conducted on FTO samples (T1, T2, T3 and T4) at different temperatures, and the absorbance was studied and the energy gaps of the samples were calculated. XRD examinations also showed the peaks of each model, FESEM images also showed the shapes of nanorods for all models. Using a photoluminescence device, it was found that the photoluminescence value was concentrated at (415 – 405 nm) in the samples prepared with TiO₂ , and its intensity was observed to decrease with increasing temperature. FTO/TiO₂ photodetectors prepared at different temperatures, where the sensitivity (140 % , 175%,315.4% and 589%) and photoresponse (0.007,0.014, 0.041and 0.171 A/W) to temperatures (150°C , 160°C ,170°C and 180°C) respectively. These parameters were calculated using ultraviolet light with a wavelength of 385 nm and an intensity of 0.05 mw/cm² at room temperature , applying a bias voltage of (1volt) , an on time of 20 seconds, and an off time of 20 seconds. These rays were shone perpendicularly to the photodetectors at a distance of 5 cm. In this study, we will focus on the best results resulting from the measurements

Keywords: Anatase and rutile phases; annealing effect TiO₂ nanorods; hydrothermal method; surface morphology.

1. Introduction

Titania (TiO₂) is one of the well-known titanium compounds that is often used in various applications. These applications include self-cleaning coatings, anti-corrosion coatings, photovoltaics, photocatalysis, photodetectors, and dye-composite solar [6]. There are three different phases of the crystal form of TiO₂: rutile, anatase (tetragonal structure), and brookite (orthorhombic structure) phases [7]. Both rutile and anatase belong to different phase groups although they have a tetragonal crystal structure. Rutile TiO₂ has higher (electrical resistivity, refractive index, chemical stability and dielectric constant) than those of the anatase phase [13]. Titanium dioxide is known to be a very useful, non-toxic, environmentally friendly, sunscreen and corrosion-resistant substance, and it is often used in white paint and pigments due to its white color. It is an n-type semiconducting material with an energy bandgap of 3.02 eV for rutile, 3.23 eV for anatase, and 3.13 eV for brookite [12]; [10]; [2], TiO₂ can be grown using many different methods Such as spraying [2], chloride process spray pyrolysis [10], chemical vapor deposition [4] and Sol-gel method [16], physical vapor deposition (PVD) and the hydrothermal method [11]. Hydrothermal synthesis is the method used to manufacture materials at low temperatures with high vapor pressure. Since the reaction occurs in closed system conditions, this method is considered the most environmentally friendly and energy-saving [15]. Teflon-lined stainless steel autoclave is usually used for hydrothermal synthesis under controllable temperature in aqueous solutions [3]. Materials manufactured by the hydrothermal method have many qualities. High purity, good homogeneity and crystalline integrity with fine grain size distribution [14]. The hydrothermal method is a successful way to prepare titanium oxide, zinc oxide and other remarkable materials [17]. In this work, TiO₂ nanofilms were synthesized using an uncomplicated hydrothermal method at reaction temperature (150°C, 160°C and 170°C) and time (4 h). The effect of high annealing temperatures (450 °C) on the structural composition, surface morphology and optical band gap was studied.

2. Experimental details

2.1. Materials and methods

Hydrochloric acid (HCl) (SDFCL, 35.4%) was used. Fluorine-doped tin oxide (FTO) conductive glass was used as a substrate for TiO₂ thin film deposition. Distilled and deionized water was used. 40 mL of hydrochloric acid was mixed with 20 mL of deionized distilled water using a magnetic stirrer for 20 minutes. Add 0.5 ml of TiO₂ to the mixture and use a magnetic stirrer for 20 minutes as well. Next, two FTO glass slices were inserted vertically into the Teflon-lined layer, which had been pre-cleaned by ultrasonography in a propanol and acetone sequence for 15 min apart. 40 ml of the prepared solution was added to a Teflon-lined stainless steel autoclave (100 ml), heated in an oven at different temperatures (150°C, 160°C, 170°C and 180°C) for 4 hours, then left to cool self-cooling until it reached... Room temperature. The substrates were removed from the autoclave, dried, and heat treated at 450 for one hour. Finally, a white layer of TiO₂ was obtained on the surface of the FTO substrate.

2.2 Characterizations

Structural characterizations of TiO₂ nanostructure films were performed using X-ray diffraction (X-Ray Diffractometer, DX-2700) with Cu K α . The scanning angle varied in the range of (10-70)° at a room temperature with a wavelength of 1.5406 Å. The surface morphologies were characterized using field mission scanning electron microscope FE-SEM (FEI FESEM Nova 450, FEI-Netherlands-Holland). The optical characterization was studied from the outcome of the absorbance and transmittance in the UV-Vis region (300-900)nm using a double beam Mega 2100-Sinco UV-Vis spectrophotometer.

Results and discussion

X-ray pattern diffraction was performed to investigate the crystalline structure of TiO₂ nanorod thin film, prepared by hydrothermal method on the fluorine-doped tin oxide (FTO) glass substrate. Table(1) shows the values of the X-ray peaks of FTO at room temperature

sample	Pos.[2Th]	Height[cts]	FWHM.[2Th]	d-spacing [Å]	Rel.int %
FTO	27.2661	33.94	0.0787	3.27080	100.00
	34.4737	13.68	0.1574	2.60169	40.31
	38.4568	16.73	0.1574	2.34089	49.29
	52.1930	24.73	0.0984	1.75259	72.84
	55.2919	3.35	0.7085	1.66148	9.87
	60.1300	2.76	0.1181	1.53885	8014
	62.1970	3.55	0.4723	1.49259	10.47
	66.0420	4.32	0.362	1.4113	10.15

Fig. 1 shows the phase of the FTO formed at room temperature. The diffraction peaks were located at $2\theta = 34.4737^\circ$, 52.1930° , 55.2919° , 62.1970° and 66.0420° belong to the (100), (211), (220), (002) and (310) surfaces respectively. These findings are in agreement with the JCPDS-41-1445 card.

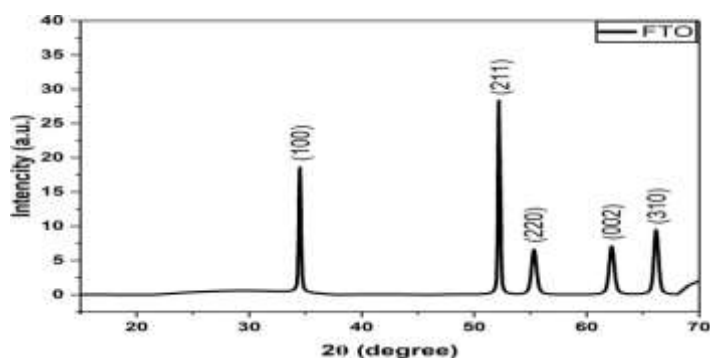
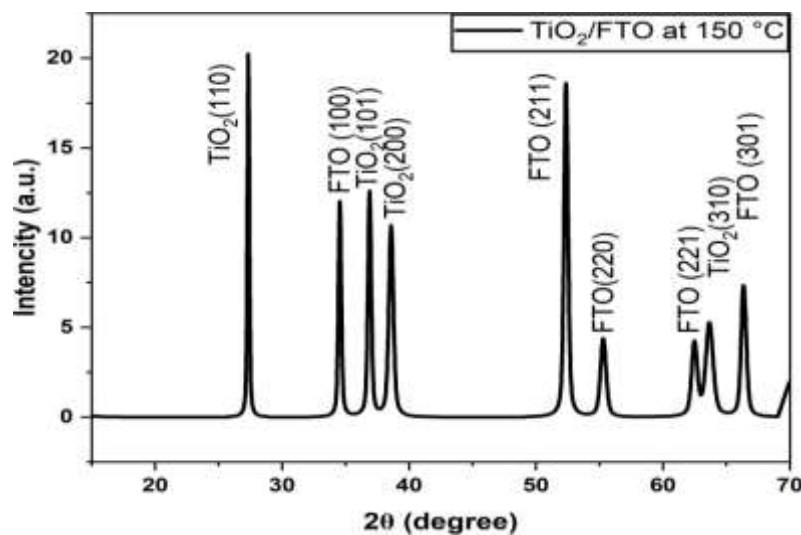


Fig. 1 shows the phase of the FTO formed at room temperature

Table. 2 shows the rutile phase of the formed TiO_2 at the 150°C preparation temperature and 4 h time .

sample	Pos.[2 θ]	Height[cts]	FWHM.[2 θ]	d-spacing [Å]	Rel.int %
TiO_2/FTO	27.3169	13.73	0.1574	3.26483	91.89
	34.4853	7.69	0.2362	2.60083	51.47
	36.8907	9.93	0.2755	2.43659	66.47
	38.5363	7.30	0.3936	2.33624	48.85
	42.0290	3.96	0.2362	2.14983	26.50
	52.2924	14.94	0.1968	1.74949	100.00
	55.2416	2.79	0.4723	1.66287	18.70
	62.4153	2.70	0.4723	1.48789	18.06
	63.6083	3.15	0.6298	1.46283	21.09
	66.3286	4.71	0.5760	1.40812	31.53

Fig. 2 shows the rutile phase of the formed TiO_2 at the 150°C preparation temperature and 4 h time. The diffraction peaks were located at $2\theta = 27.3169^\circ, 34.4737^\circ, 36.8907^\circ, 38.5363^\circ, 52.2924^\circ, 55.2416^\circ, 62.4153^\circ, 63.6083^\circ$ and 66.3286° belong to the (110), (100), (101), (200), (211), (220), (221), (310) and (301). These findings are in agreement with the JCPDS-21-1276 card. Small FWHM indicates that the crystallinity of the TiO_2 nano crystal was fairly high.



. Fig. 2 shows the rutile phase of the formed TiO_2 at the 150°C preparation temperature and 4 h time

Table. 3 shows the rutile phase of the formed TiO_2 at the 160°C preparation temperature and 4 h time .

sample	Pos.[2 θ]	Height[cts]	FWHM.[2 θ]	d-spacing [Å]	Rel .int %
TiO_2/FTO	12.7367	0.17	3.7786	6.95041	0.51
	27.2564	13.60	0.1181	3.27195	40.48

	29.0375	2.26	0.1968	3.07518	6.73
	32.7143	2.12	0.2362	2.73747	6.32
	34.4747	5.91	0.2362	2.60161	17.61
	36.7912	11.81	0.1574	2.44295	35.15
	38.4936	3.93	0.2362	2.33874	11.69
	52.1672	14.56	0.1181	1.75340	43.36
	55.2289	1.75	0.9446	1.66322	5.20
	62.2756	2.85	0.4723	1.49089	8.50
	63.4366	33.59	0.0984	1.46637	100.00
	66.3160	5.06	0.4800	1.40835	15.05

. Fig. 3 shows the rutile phase of the formed TiO_2 at the 160°C preparation temperature and 4 h time. The diffraction peaks were located at $2\theta = 27.2, 34.4, 36.7, 38.4, 52.16, 55.2289, 62.2756, 63.4$ and 66.3 and corresponding to the following crystalline levels (110), (100), (101), (200), (211), (220), (221), (310) and (301) respectively. Where the peaks belong (100), (211), (220), (221) and (301) to the base of FTO As for the remaining vertices, they correspond to TiO_2 . The rutile phase has a quadrilateral rhombus, as observed from the top (110), (101), (200) and (310).

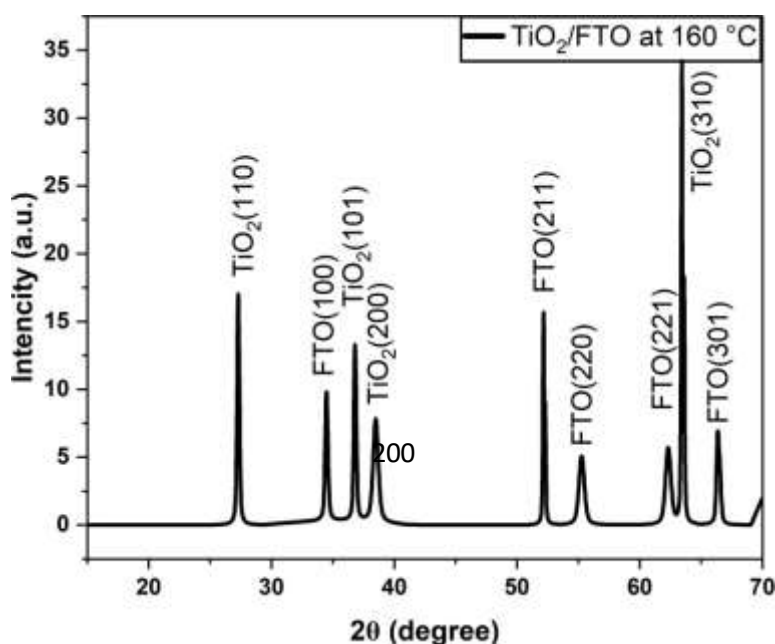


Fig.3 shows the rutile phase of the formed TiO_2 at the 160°C preparation temperature and 4 h time

Table. 4 shows the rutile phase of the formed TiO_2 at the 170°C preparation temperature and 4 h time

sample	Pos.[2Th]	Height[cts]	FWHM.[2Th]	d-spacing [Å]	Rel .int %
TiO2/FTO	11.4861	0.98	2.5190	7.70417	7.51
	16.2705	1.13	0.7872	5.44791	8.70

	23.9706	0.44	0.3936	3.71248	3.38
	27.3254	10.75	0.1574	3.26383	82.47
	34.5375	9.25	0.1181	2.59702	70.92
	36.8985	13.04	0.2362	2.43609	100.00
	38.5127	6.00	0.2362	2.33762	46.01
	41.9727	2.19	0.3936	2.15258	16.80
	52.3343	11.23	0.3149	1.74819	86.12
	55.1742	3.97	0.4723	1.66474	30.42
	63.5464	7.19	0.2755	1.46411	55.12
	66.2857	5.20	0.2880	1.40892	39.85

. Fig. 4 Shows the rutile phase of the formed TiO_2 at the 170°C preparation temperature and 4 h time. The diffraction peaks were located at $2\theta = 27.3245$, 34.5375 , 36.8985 , 38.5127 , 52.3343 , 55.1742 , 63.5464 and 66.2857 belong to the (110) , (100) , (101) , (200) , (211) , (220) , (310) and (301) surfaces respectively.

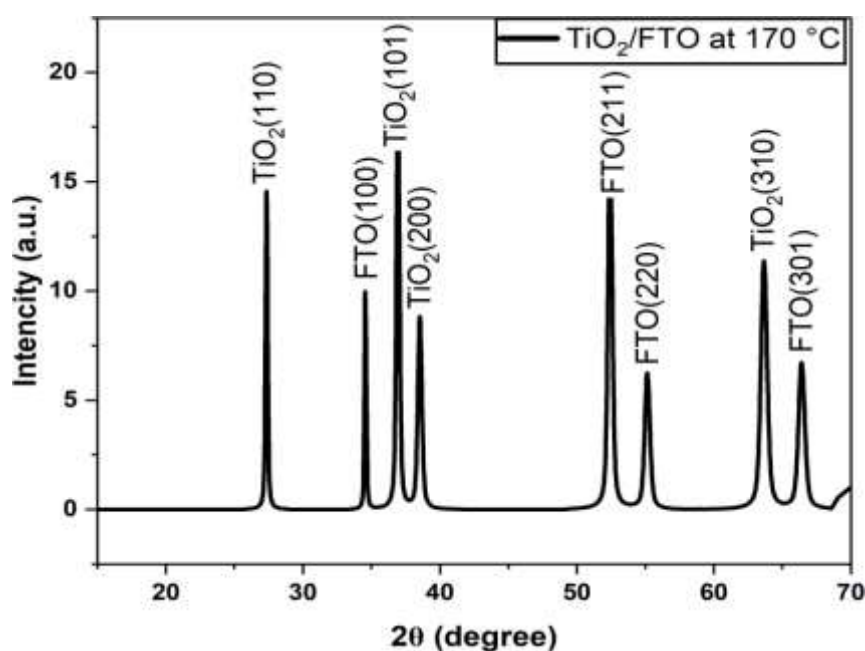


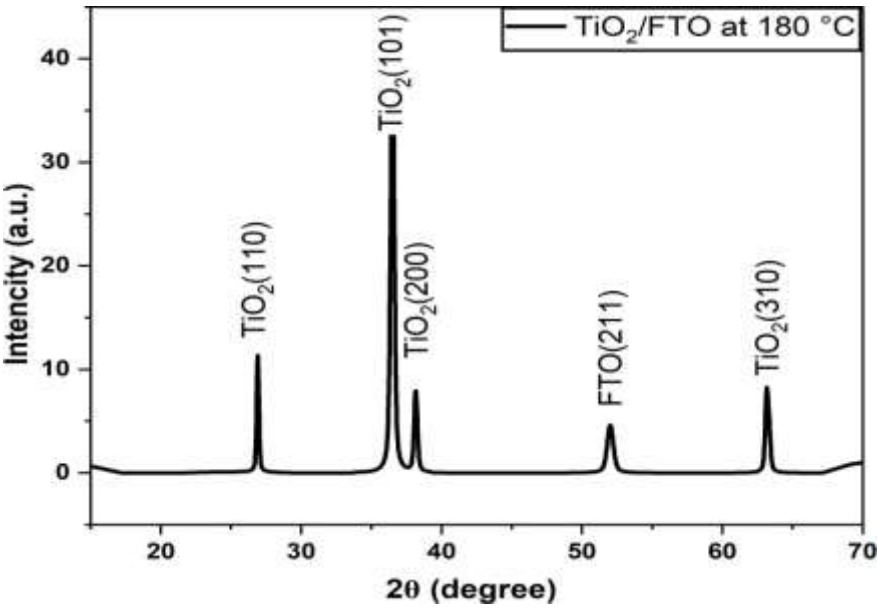
Fig. 4 Shows the rutile phase of the formed TiO_2 at the 170°C preparation temperature and 4 h time

Table. 5 shows the rutile phase of the formed TiO_2 at the 180°C preparation temperature and 4 h time .

sample	Pos.[2Th]	Height[cts]	FWHM.[2Th]	d-spacing [Å]	Rel .int %
TiO2/FTO	26.8762	7.85	0.1574	3.31735	26.51
	36.4474	29.60	0.1181	2.46520	100.00
	38.1522	5.21	0.2755	2.35888	17.61

	51.9187	2.49	0.6298	1.76120	8.41
	63.1962	5.32	0.2880	1.47015	17.96

. Fig.5 Shows the rutile phase of the formed TiO₂ at the 180 C⁰ preparation temperature and 4 h time. The diffraction peaks were located at 2θ =26.8762, 36.4474, 38.1522, 51.9187and 63.1926 belong to the (110) , (101) , (200) , (211) and (310) surfaces respectively.



. Fig. 5 Shows the rutile phase of the formed TiO₂ at the 180 C⁰ preparation temperature and 4 h time.

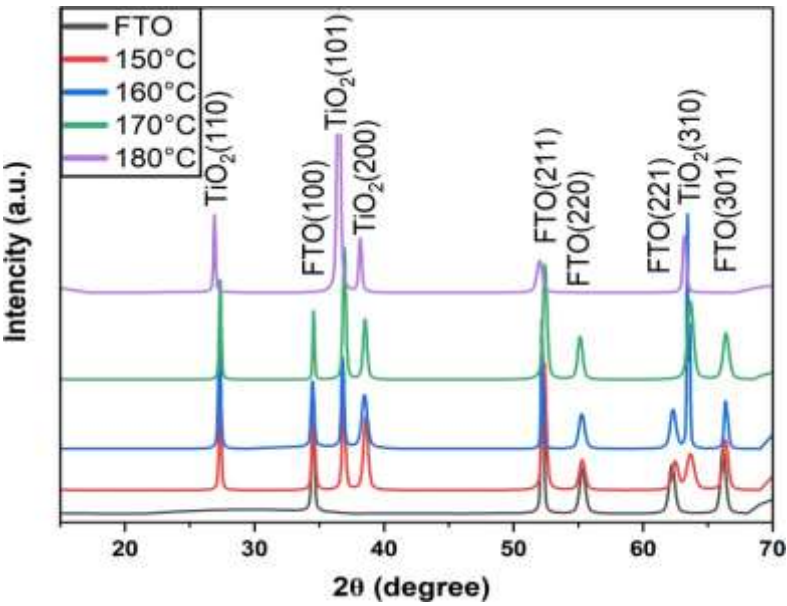
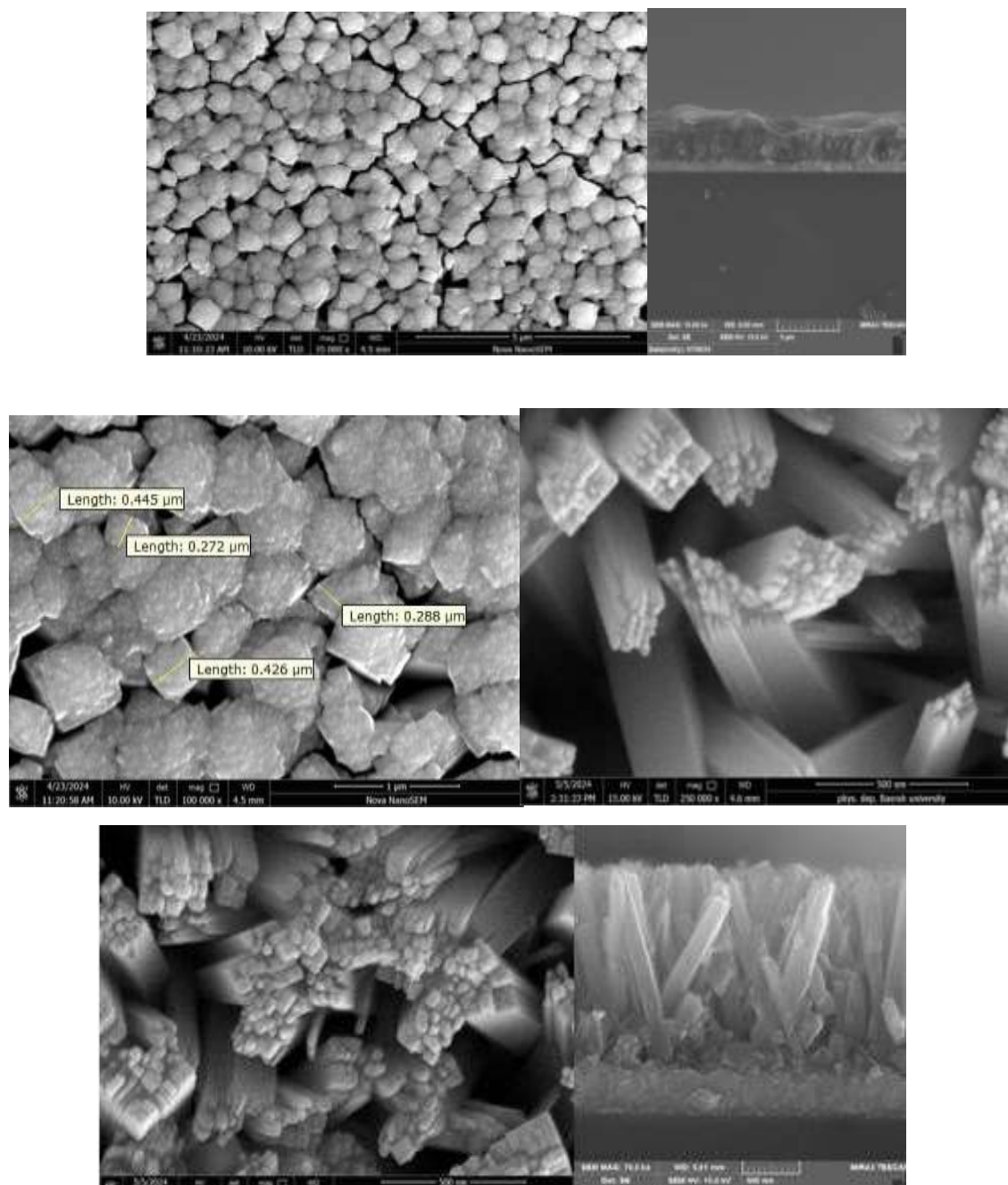


Fig. 6 shows the XRD for TIO2/FTO at different temperatures

Microscopic images of TiO_2 nanostructures obtained from field emission scanning electron microscopy (FESEM) on FTO substrates prepared at different temperatures are illustrated (150°C , 160°C , 170°C and 180°C) and hardened (450°C). Figure (7) shows the microscopic image of TiO_2 nanostructures prepared by hydrothermal method at (150°C , 160°C , 170°C and 180°C) and annealed at (450°C). Microscopic images reveal that TiO_2 has a nanostructure with a quadrangular shape. Figure (7) SEM Images of TiO_2 Film on TiO_2/FTO prepare at ($150-180$) $^\circ\text{C}$ The film image at 150°C shows TiO_2 and it looks like a nanorod with a diameter of approx (272-445) nm. And the cross-section of TiO_2 film, which has a length about 347nm, The film image at 160°C shows TiO_2 and it looks like a nanorod with a diameter of approx (139 - 239) nm, The film image at 170°C shows TiO_2 and it looks like a nanorod with a diameter of approx (84 - 270) nm The film image at 180°C shows TiO_2 and it looks like a nanorod with a diameter of approx (129 - 286) nm. And the cross-section of TiO_2 film, which has a length about (1803)nm.,



. Fig. 7 SEM Images of TiO_2 Film on TiO_2/FTO prepare at ($150-180$) $^\circ\text{C}$

UV and visible transmittance spectra were studied to study the effect of deposition temperature on the absorption edge of TiO₂. Figures (8 - 11) show the optical transmittance (TiO₂/FTO energy gap) and optical absorption spectra corresponding to the Tauc relationship [1]. The optical properties of nanostructured thin films were studied using absorbance spectroscopy over the wavelength range (320-800). Whereas, the absorption spectra of TiO₂ composite films prepared by the hydrothermal method and at different strong temperatures in the UV region (150 oC , 160 oC , 170 oC , 180 oC) show weak absorption in the visible region, which indicates that they are violet between (300-400 nm). It has a wide energy gap, and absorption increases with increasing temperature. When temperatures rise, high absorption is observed in the visible region $\lambda < 410$, which is generally associated with absorption. Visible light through surface defects of TiO₂. The energy gap was calculated for example for the membranes and prepared using the transmission spectrum as shown in the figure from its diagram $(\alpha h\nu)^2 \cdot (h\nu)$ by extrapolating the straight line of the curve to intersect with the photon energy axis at $(\alpha h\nu)^2$. We notice a slight difference in the value of the energy gap. This difference is due to the difference in the nanorod size of the thin films depending on the increase in concentration and deposition temperature. And it may be so. Increased crystallinity and regularity in the crystalline structure of the thin layer is also one of the reasons. When calculating, we notice that the energy gap decreases upon annealing due to the improvement in the size of the heat-treated grains. The edge of absorbance (It is a sudden increase in the degree of absorption of electromagnetic radiation by a substance with an increase in the radiation frequency. Absorption edges are characteristic of X-ray behavior and are related to the precisely defined energy levels occupied by electrons in atoms) appear about 410 nm. The energy gap can be calculated using the equation

$$E_g = 1240/\lambda \quad (1)$$

The band gap 3eV at 180°C⁰. While the energy gaps were (2.4eV, 2.5eV and 2.7eV) at temperatures (150 °C , 160 °C and 170 °C) respectively The energy gap values were less than 3 eV; It could be due to the narrowing of the band gap caused by the presence of structural defects in the composite TiO₂ nanorods. Smaller crystal size and particle size increase the ratio of surface defects to bulk defects, thus increasing conduction and valence band residues, leading to a narrower band gap [5].

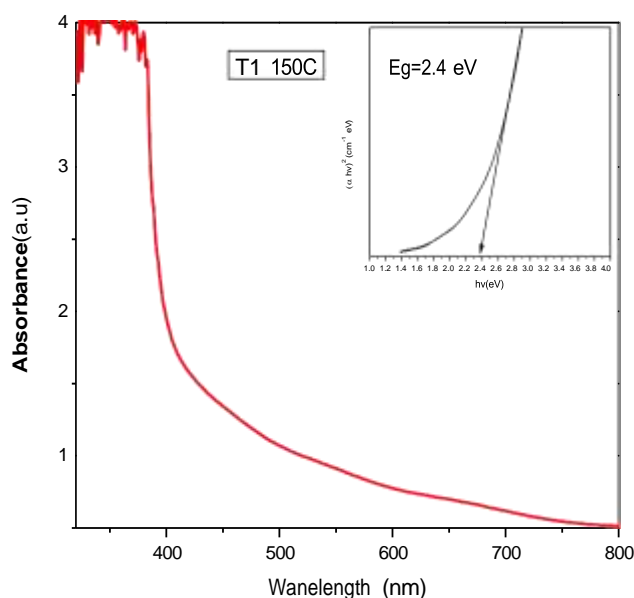


Fig. 8 Absorbance in TiO₂ at 150°C

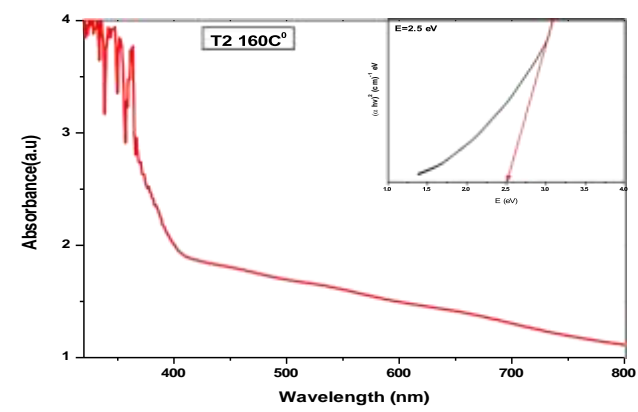


Fig.9 Absorbance in TiO₂ at 160C⁰

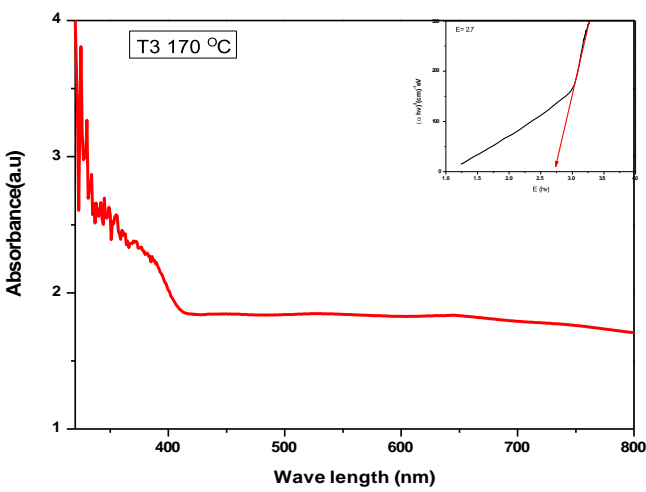


Fig.10 Absorbance in TiO₂ at 170C⁰

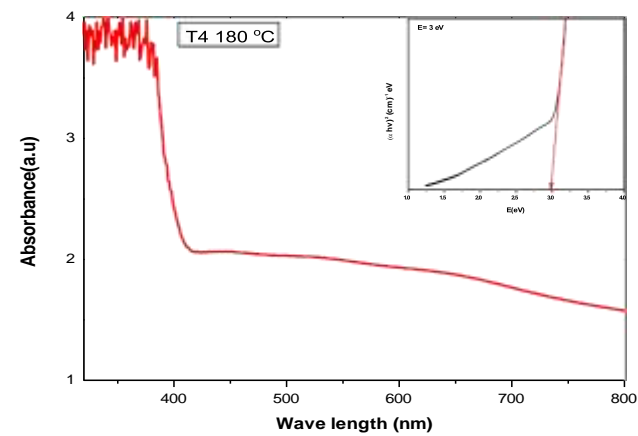
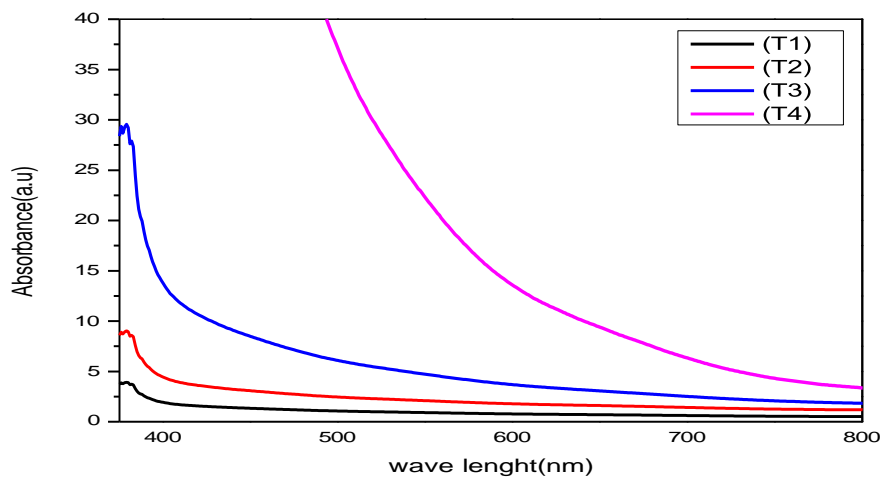


Fig.11 Absorbance in TiO_2 at 180°C Fig.12 shows Absorbance in TiO_2 at different temperatures

We can also show the relationship between the energy gap and temperature through the following figure (13)

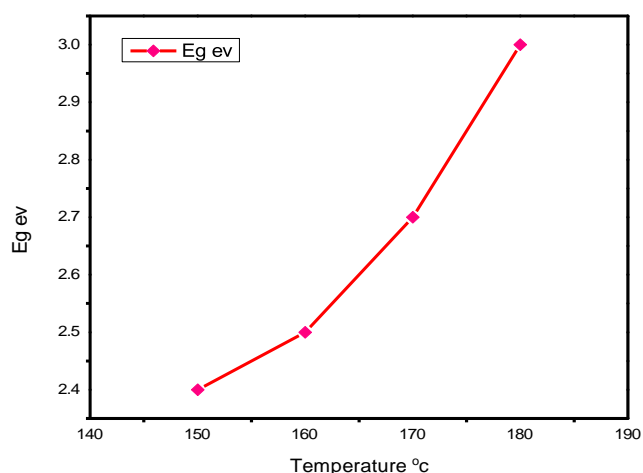


Fig. 13 show the relationship between the energy gap and temperature

Photoluminescence (PL) or instantaneous luminescence is a phenomenon in which a particular substance emits light after it absorbs light or electromagnetic energy. When a substance is exposed to light, the electrons in the atoms and molecules of the substance move to a higher energy level. When these electrons return to lower energy levels, the energy is released in the form of photons, causing fluorescence. Photoluminescence spectrum of room temperature TiO_2 films prepared on FTO bases using the hydrothermal method at different temperatures (150°C , 160°C , 170°C , and 180°C). Using an excitation wavelength of 330 nm, the spectra show an emission peak, i.e., upon excitation with band gap energy, the photoexcited electrons drop to a minimum in the excited state [8]. When TiO_2 is exposed to light, it rebuilds an electron hole and emits light photons [9]. Figure (14) appears to be a plot of intensity versus wavelength, likely from a spectroscopic measurement. The y-axis is labeled intensity (count sec⁻¹) and the x-axis is labeled wavelength (nm). The plot is titled (T1) FTO at 150°C . The emission peak appears about 415 nm in the intensity 500 (count sec⁻¹). The energy gap can be calculated using the equation (1). The band gap 2.987 eV the plot is titled (T2) FTO at 160°C . The emission peak appears about 410 nm in the intensity 390 (count sec⁻¹), The energy gap. The band gap 3.02 eV

. The plot is titled (T3) FTO at 170°C , The emission peak appear about 405 nm in the intensity 350(count sec⁻¹), The band gap 3.06 eV. The plot is titled (T4) FTO at 180°C . The emission peak appear about 405 nm in the intensity 550(count sec⁻¹), The band gap 3.06 eV.

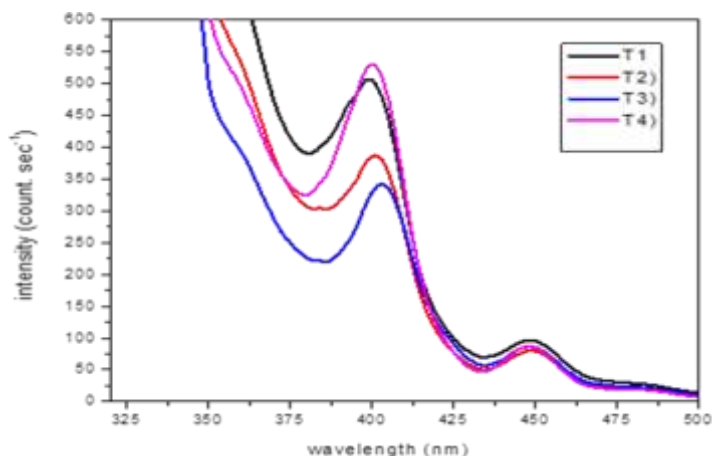


Fig 14 the photoluminescence for FTO at different temperatures

current – voltage characteristics Among the electrical characteristics through which the performance of the photodetector is described are the characteristics (current - voltage), which shows the behavior of the current with the voltages applied to the detector. The electrical properties of photodetectors were studied in the dark and in the presence of light, and the use of the Keithley 2400 device under a forward bias voltage of 1 volt. Figure (15) shows the change in the amount of electrical current with a change in temperature, with a constant bias voltage value, an on time of 20 seconds, and an off time of 20 seconds, using ultraviolet light with a wavelength of 385 nm and an intensity of 0.05 mW/cm² at room temperature. These rays were directed vertically on The sample is at a distance of (5 cm), where an increase in the electric current values was observed with the change in temperature, as the value of the current increases with the increase in temperature relative to photodetectors.

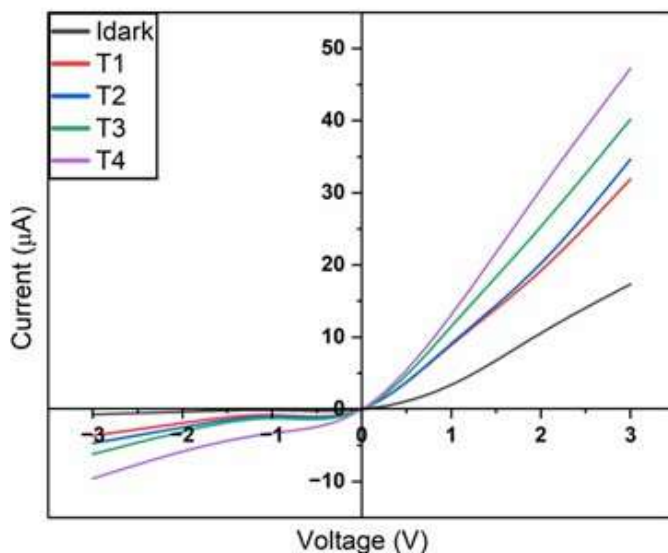


Fig. (15) shows the change in the amount of electrical current with a change in temperature .

Photoresponse measurements of TiO₂/FTO photodetectors prepared by the hydrothermal method were performed at different temperatures, using UV light with a wavelength of 385 nm and an intensity of 0.05 mW/cm² at room temperature, a bias

voltage of 1 volt , and an operation time of 20 seconds. And an extinguishing time of 20 seconds. These rays were directed vertically at the photodetectors at a distance of 5cm, and the optical response and sensitivity were calculated using equations

$$R_{\lambda} = \frac{I_{ph}}{P_{in}} \quad (2)$$

$$S = \frac{I_{ph} - I_{dark}}{I_d} * 100\% \quad (3)$$

. It has been found that the work of photodiodes is to generate electron gap pairs by absorbing incident light. The rise time was then calculated, which means the response time of the photodetector with a time difference between 10% and 90% of the maximum optical current. In addition to calculating the fall time, the results at figure (16) were as follows:

The first model, T1 (TiO₂/FTO), prepared at a temperature of 150oC, had a rise time of 33.6 s, a fall time of 36.5 s, a dark current of 0.05 μ A, a photocurrent of 0.12 μ A, a sensitivity of 140%, a photoresponse of 0.007 A/W, and an efficiency of 2.3%.

The second model, T2 (TiO₂/FTO), prepared at a temperature of 160oC, had a rise time of 32.1 s, a fall time of 38.4 s, a dark current of 0.08 μ A, a photocurrent of 0.22 μ A, a sensitivity of 175%, a photoresponse of 0.014 A/W, and an efficiency 4.5 %

The third model, T3 (TiO₂/FTO), prepared at a temperature of 170oC, had a rise

time of 33.7 s, a fall time of 42 s, a dark current of 0.13 μ A, a photocurrent of 0.54 μ A, a sensitivity of 315.5%, a photoresponse of 0.041 A/W, and an efficiency of 13.2 % .

The fourth model, T4 (TiO₂/FTO), prepared at a temperature of 180oC, had a rise time of 24.9 s, a fall time of 31.3 s, a dark current of 0.29 μ A, a photocurrent of 2 μ A, a sensitivity of 589.7%, a photoresponse of 0.171 A/W, and an efficiency of 55.2 % .

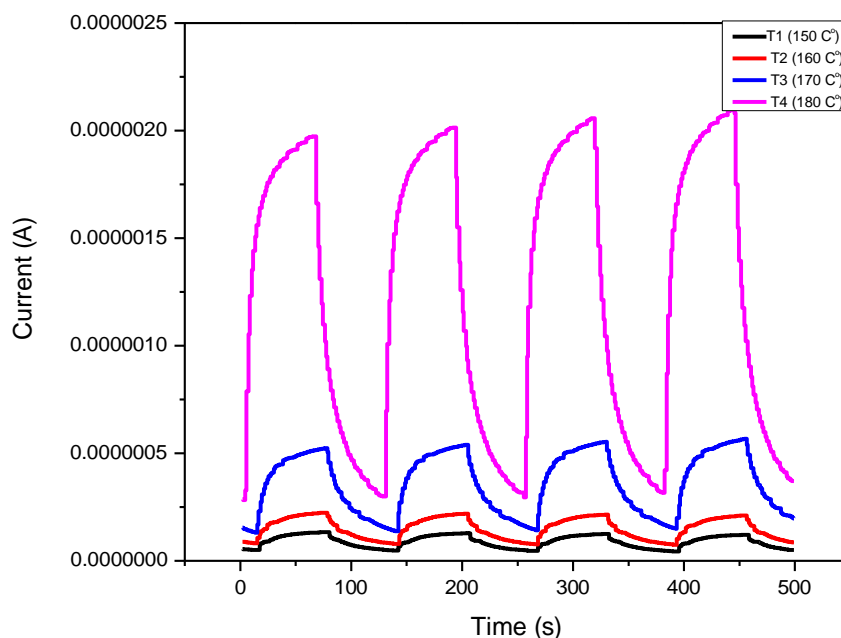


Fig. 16 Time response of the detector T4 (TiO₂/FTO) at 180oC

sample	Temperature	T _{rise} (s)	T _{fall} (s)	I _{dark}	I _{ph}	Sph%	R(A/W)	η%
--------	-------------	-----------------------	-----------------------	-------------------	-----------------	------	--------	----

T1	150 °C	33.6	36.5	0.05	0.12	140	0.007	2.3
T2	160 °C	32.1	38.4	0.08	0.22	175	0.014	4.5
T3	170 °C	33.7	42	0.13	0.54	315.4	0.041	13.2
T4	180 °C	24.9	31.3	0.29	2	589.7	0.171	55.2

Tabl (7) Shows the results of photodetectors at different temperatures

4- Conclusion

TiO₂ nanorods were successfully synthesized on FTO conductive glass substrate by the hydrothermal method. The deposition parameters and conditions were as follows: Hydrochloric acid (HCl) (SDFCL, 35.4%) was used. Fluorine-doped tin oxide (FTO) conductive glass was used as a substrate for TiO₂ thin film deposition. Distilled and deionized water was used. 40 ml of hydrochloric acid was mixed with 20 ml of deionized distilled water using a magnetic stirrer for 20 minutes. Add 0.5 ml of TiO₂ to the mixture and use a magnetic stirrer for 20 minutes as well

TiO₂ nanorods were arranged in the xz plane, i.e., they prefer to grow in the plane (101) of the tetragonal anatase TiO₂ crystal. XRD results show the successfully fabricated TiO₂ nanorods with the desired size and preferential anatase phase using titanium btoxide as a starting material. . The obtained results indicate that TiO₂ material is very suitable for photovoltaics and photocatalysis applications.

ACKNOWLEDGEMENTS

The authors are very grateful for the assistance provided by the Department of Physics, College of Science, University of Basra, Iraq, Professor Dr. Sattar Jabbar Qasim, Department of Physics, College of Science, University of Basra, Assistant Professor Dr. Alaa Abdel Halim, College of Science, University of Basra, and PhD student Mr. Ghaith Abdel Razzaq, College of Science, University of Basra.

References

- [1] **Alkhayatt, A.; Habieb, A.; Al-Noaman, A., and Hameed, A. (2019).** Structure, surface morphology, and optical properties of CuxZn1- xS/Au NPs layer for photodetector application The 1st International Scientific Conference on Pure Science IOP Conf. Series: Journal of Physics: Conf. Series 1234: 012012.
- [2] **Bedikyan, L.; Zakhariev, S. and Zakharieva, M. (2013).** Titanium Dioxide Thin Films: Preparation and Optical properties. (2013). J. Chem. Technol. Metall. **48**: 555-558.
- [3] **Bregadiolli, B.; Fernandes, S. and Graeff, C. (2017).** Easy and Fast Preparation of TiO₂ based Nanostructures Using Microwave Assisted Hydrothermal Synthesis. Materials Research, 20(4): 912-919.
- [4] **Byranvand, M.; Kharat, A.; Fatholahi, L., and Beiranvand Z. (2013).** A Review on Synthesis of Nano-TiO₂ via Different Methods J. nanostructures **3**: 1-9.
- [5] **El-Sayed, A.; Atef, N.; Hegazy, A.; Mahmoud, K.; Abdel Hameed, R. et al. (2017).** Defect states determined the performance of dopant-free anatase nanocrystals in solar fuel cells. Solar Energy **144**: 445–452.
- [6] **Keerthana, B.; Solaiyammal, T.; Muniyappan, S.; and P Murugakoothan, P. (2018).** Hydrothermal synthesis and characterization of TiO₂ nanostructures prepared using different solvents. Mater. Lett. 220: 20-23.
- [7] **Khataee, A., and Mansoori G., (2011)** Nanostructured Titanium Dioxide Materials (World Scientific Publishing Company), p 4.
- [8] **Mart M Rajabi, S ShoghJournal of Luminescence, 2015•Elsevier** Defect study of TiO₂ nanorods grown by a hydrothermal method through photoluminescence spectroscopy

- [9] **M Vishwas, KN Rao, RPS Chakradhar Spectrochimica Acta Part A: Molecular and Biomolecular Spectroscopy, 2012** Influence of annealing temperature on Raman and photoluminescence spectra of electron beam evaporated TiO₂ thin films
- [10] **Oja, I.; Mere, A.; Krunks, M.; Solterbeck C. and M Souni. (2004).** Properties of TiO₂ Films Prepared by the Spray Pyrolysis Method. Solid State Phenomena 99-100: 259-264 (2004).
- [11] **Palmisano, L.; Augugliaro, V.; Sclafani, A. and M Schiavello. (1988).** Activity of chromium-ion-doped titania for the dinitrogen photoreduction to ammonia and for the phenol photodegradation. J. Phys. Chem., 92: 6710-6713.
- [12] **Tang, H.; Levy, F.; Berger, H. and Schmid, P. (1995).** Urbach tail of anatase TiO₂. Phys. Rev. B 52: 7771-7774.
- [13] **Tsevis, A.; Spanos, N.; Koutsoukos, P.; A. Linde, A. J. and Lyklema, J. (1998).** Preparation and characterization of anatase powders. J. Chem. Soc. Faraday Trans. 94 (2): 295-300.
- [14] **Wirunmongkol, T.; O-charoen, N. and Pavasupree, S. (2013).** Simple Hydrothermal Preparation of Zinc Oxide Powders Using Thai Autoclave Unit. Energy Procedia **34**: 801-807.
- [15] **Zheng, S.K. (2016)** First-principles calculations of Ca/F co-doped anatase TiO₂. Kuwait J. Sci., **43** (2): 162-171.
- [16] **Serrano, E., Linares, N., Garcia-Martinez, J., & Berenguer, J. R. (2013).** Sol–Gel Coordination Chemistry: Building Catalysts from the Bottom-Up. ChemCatChem, 5(4), 844-860.
- [17] **Chennakesavulu, K., Reddy, M. M., Reddy, G. R., Rabel, A. M., Brijitta, J., Vinita, V., ... & Sreeramulu, J. (2015).** Synthesis, characterization and photo catalytic studies of the composites by tantalum oxide and zinc oxide nanorods. Journal of Molecular Structure, 1091, 49-56